Energy Partition in Nuclear Fission

A. Ruben, H.Märten, and D.Seeliger
Technische Universität Dresden, Sektion Physik
Mommsenstr.13, DDR-8027, German Democratic Republic

Abstract - *A scission point model (two spheroid model TSM) including semi-empirical temperature-dependent shell correction energies for deformed fragments at scission is presented. It has been used to describe the mass-asymmetry-dependent partition of the total energy release on both fragments from spontaneous and induced fission. Characteristic trends of experimental fragment energy and neutron multiplicity data as function of incidence energy in the Th-Cf region of fissioning nuclei are well reproduced. Based on model applications, information on the energy dissipated during the descent from second saddle of fission barrier to scission point have been deduced.*

I. INTRODUCTION

The progress achieved in nuclear fission theory have led to a qualitative understanding of most of known fission characteristics[1]. However, it fails to reproduce experimental fission data with adequate quantitative accuracy in a global manner, in particular the dependence of fission observables on excitation energy E_{cn} of the fissioning nucleus (including spontaneous fission, i.e. E_{cn}=0). One of the important questions with relevance to applications, e.g. nuclear data evaluation for actinides, is the problem of partition of total available energy (as the sum of Q-value and E_{cn}) on both complementary binary-fission fragments.

The well-known neutron multiplicity saw-tooth $\bar{\nu}(A)$ depending on fragment mass number A, which can not be understood in the framework of the liquid drop model LDM[2], has been discussed as due to shell effects by Brunner and Paul[3] and later by Vandenbosch[4].

Terrell[5] proposed a simple model to describe fission energetics as function of mass asymmetry A_1/A_2. Idealizing the scission configuration by two spheroidically shaped fragments with major semi-axis D_i, the deformation-dependent part of the potential has been minimized leading to simple expressions for describing the energy partition. The crucial parameter is the deformability α (a measure of stiffness) strongly influenced by shell effects. Based on Terrell's approach Kildir and Aras[6] studied fission energy partition for ^{252}Cf(sf). Using Myer's and Swiatecki's[7] shell correction energies δw they adjusted an empirical relation for describing α as function of δw. Corresponding α values were deduced from experimental quadrupole moments.

The static scission point model proposed by Wilkins et al.[8] is suitable to explain most of the fission characteristics. Shell and pairing effects are considered for deformed fragments (spheroids) as function of intrinsic temperature. Statistical equilibrium is separately accounted for collective degrees of freedom yielding a "collective" temperature.

The assumption of statistical equilibrium at scission was declined by Brosa[9]. His random-neck-rupture model accounts for a fissioning nucleus with a rather long neck connecting the two nascent fragment volumes. The neck cut-up is chosen randomly. This semi-stochastic approach including Raleigh's instability criterion gives a fair description of observable averages as well as width's. However, one should keep in mind that the most probable neck cut up position is determined by statics. It differs for various fission modes which are already visible in the potential energy surface.

The aim of the present work is to give a simple (and easily applicable) model for the description of average fragment energies, i.e. total kinetic energy $\overline{TKE}(A_1/A_2)$ and excitation energy $\bar{E}^*(A)$, in spontaneous as well as induced fission. Starting with a general energy balance Terrell's approach has been generalized by the incorporation of most important microscopic effects.

The model is applied to study fragment energies as function of incidence energy in comparison with experimental data. Note that $\bar{\nu}$ data are a measure of $\bar{E}^*$. Most emphasis is put to reproduce striking trends of fragment energy data in the Th - Pu region.

II. GENERAL ENERGY BALANCE IN INDUCED FISSION

Before describing the scission point model, general relations to account for the energy balance in induced fission are outlined. Fig. 1 represents a scheme of main energy values which are

important during the fission process starting at compound-nucleus excitation of energy E_{cn} and passing the double-humped fission barrier with the heights $E_{f,A}$ and $E_{f,B}$ as well as the scission point. We describe the scission point energy parts with reference to saddle B. Here, the intrinsic excitation energy is assumed to be

$$E_h = E_{cn} - E_{f,B} - \Delta_p \qquad (1)$$

with the constraint $E_h \geq 0$, i.e. E_h vanishes in the case of spontaneous and subbarrier fission. Δ_p is the pairing gap above barrier B. Its intrinsic temperature dependence is calculated according to Kristiak[10].

The potential energy release between second saddle and scission point, i.e. ΔE_{pot} is assumed to be the sum of pre-scission kinetic energy E_{pre} and dissipative energy E_{dis}. The sum $E_{dis}+E_h$ corresponds to the total intrinsic energy at scission point (E_{int}). E_{int} is distributed on the complementary fragments according to statistical assumptions (equal intrinsic temperatures, cf. paragraph 3). The basic energy balance equation

$$\bar{Q}\left(\frac{A_1}{A_2}\right) + E_{cn} = \underbrace{E_{pre} + \overbrace{E_{coul}\left(\frac{A_1}{A_2}\right)}^{F\left(\frac{A_1}{A_2}\right)} + E_{def}^{(1)} + E_{def}^{(2)}}_{\overline{TKE}\left(\frac{A_1}{A_2}\right)} + \underbrace{\overbrace{E_{dis} + E_h}^{E_{int}^{(1)}+E_{int}^{(2)}}}_{\bar{E}^*\left(\frac{A_1}{A_2}\right)} \qquad (2)$$

E_{coul} - Coulomb potential energy at scission,

$E_{def}^{(i)}$ - deformation energy of fragment i at scission,

E_{dis} - dissipative energy

$E_{int}^{(i)}$ - intrinsic excitation of fragment i at scission,

E_h - intrinsic excitation energy ("heat") at second saddle

F - potential energy at scission for given mass asymmetry

E_{pre} - pre-scission kinetic energy,

describes the partition of total available energy, i.e. sum of

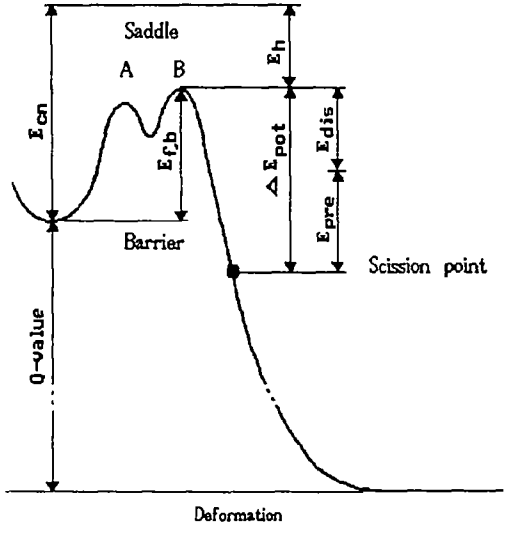

Fig.1 Potential scheme in the case of induced fission

average Q-value and fissioning nucleus excitation energy, on both fragments. E_{coul} is the coulomb potential at scission, E_{def} is the deformation energy. The "asymptotic" excitation energy of a single fragment, i.e. after dissipation of deformation energy into intrinsic energy but before de-excitation, is obtained by

$$\bar{E}^*(A_i) = E_{def}^{(i)} + E_{dis}^{(i)} \qquad (3)$$

Further, the total kinetic energy of fission fragments for given mass number ratio is given by

$$\overline{TKE}(A_1/A_2) = E_{coul}(A_1/A_2) + E_{pre} \qquad (4)$$

F denotes the deformation-dependent part of scission point potential specified in paragraph 3.

III. THE TWO-SPHEROID-MODEL

According to Terrell[5] we describe the fissioning system by two spheroidically shaped fragments nearly touching at the scission point. The nuclear forces between the fragments cause a small distance $d \approx 1.4$ fm[6]. E_{coul} is assumed to be the coulomb repulsion

energy of two charges effectively located at the centers of the fragments, i.e.

$$E_{coul} = Z^{(1)}Z^{(2)}e^2/(D^{(1)}+D^{(2)}+d) \quad . \tag{5}$$

The deformation energy is taken to be quadratic in radius change with reference to a spherical nucleus with radius $R^{(i)}$

$$E_{def}^{(i)} = \alpha^{(i)} \, (D^{(i)}-R^{(i)})^2 \tag{6}$$

($D^{(i)}$ - major semi-axis of spheroid i, $\alpha^{(i)}$ is the deformability parameter of fragment i). Minimizing the nuclear potential F in deformation space the most probable scission configuration is found. Adopting $\partial F/\partial D^{(i)}=0$ one gets a set of equations

$$E_{def}^{(i)} = \frac{E_{coul}^4}{4 \, \alpha^{(i)} \, Z^{(1)2} \, Z^{(2)2} \, e^2} \tag{7}$$

$$E_{def}^{(1)}/E_{def}^{(2)} = \alpha^{(2)}/\alpha^{(1)} \quad . \tag{8}$$

As shown by Terrell[5], the deformability parameter $\alpha^{(i)}$ is related to the stiffness parameter $C_2^{(i)}$ (quadrupole deformation) as

$$C_2^{(i)} = \frac{5}{2\pi} \, \alpha^{(i)} \, R^{(i)2} \tag{9}$$

Consequently, the deformability parameter $\alpha^{(i)}$ can be deduced in the framework of the Liquid-Drop Model[5] (LDM). However nuclear stiffness is strongly influenced by shell effects. In order to calculate effective shell correction energies $\delta w(A)$ for fragments with typical deformations at scission the following semi-empirical relation according to Kildir and Arras[6] is used,

$$\alpha(A) = \alpha_{LDM}(A) \, \frac{K-\delta W(A)}{K+\delta W(A)} \tag{10}$$

K is a constant determined by a fit of experimental stiffness data: K= (8.0 $\pm$ 0.1) MeV.

IV. PHENOMENOLOGICAL SHELL CORRECTION ENERGIES

One possible way to apply the formalism shown above is to calculate semi-empirical, i.e. effective, shell correction energies on the basis of well known fragment data. However, it should be emphasized that shell effects are washed out by intrinsic excitation. The diminution of shell correction energies due to intrinsic temperature τ at scission can roughly be described using the Bohr-Mottelson[11] relation

$$\delta w(A,\tau) = \delta w(A,\tau=0) \, \frac{t^2 \, \sinh^2 t}{\cosh t} \tag{11}$$

with

$$t = \frac{2 \, \pi^2}{\hbar \, \omega_{sh}} \, \tau \tag{12}$$

($\hbar\omega_{sh} \simeq 25 \, A^{-1/3}$ - shell energy distance[11]). According to the general energy balance (paragraph 2) the intrinsic excitation energy E_{int} includes both dissipative energy E_{dis} and heat energy above the second fission barrier E_h. The partition on the fragments is defined by the condition of equal intrinsic temperatures τ of complementary fragments at scission ($\tau^{(1)}=\tau^{(2)}$). Thus $\tau^{(i)}$ can be calculated on the basis of the Fermi-gas model approach,

$$E_{int}^{(i)}(A) = a^{(i)}(A) \, \tau^2 \tag{13}$$

The level density parameter $a^{(i)}(A)$ is described applying the Ignatyuk formalism[12] including shell effects.

Fig.2 shows the calculated phenomenological shell correction energies reduced to zero excitation at scission (τ=0) for different fission reaction. Note that these energies are very close to each other in the most probable mass region.

On the other hand, these data agree with the Strutinski-type shell energies[8] quite well. Note that the shell correction energies depicted above are only effective phenomenological quantities for fragments with averaged properties (charge, deformation, fragment energies...) without microscopic foundation.

To apply the TSM to any fission reaction a set of most reliable shell correction energies (τ=0) for $^{235}U(n_{th},f)$ and $^{252}Cf(sf)$ were determined. Interpolating these parameters and considering the

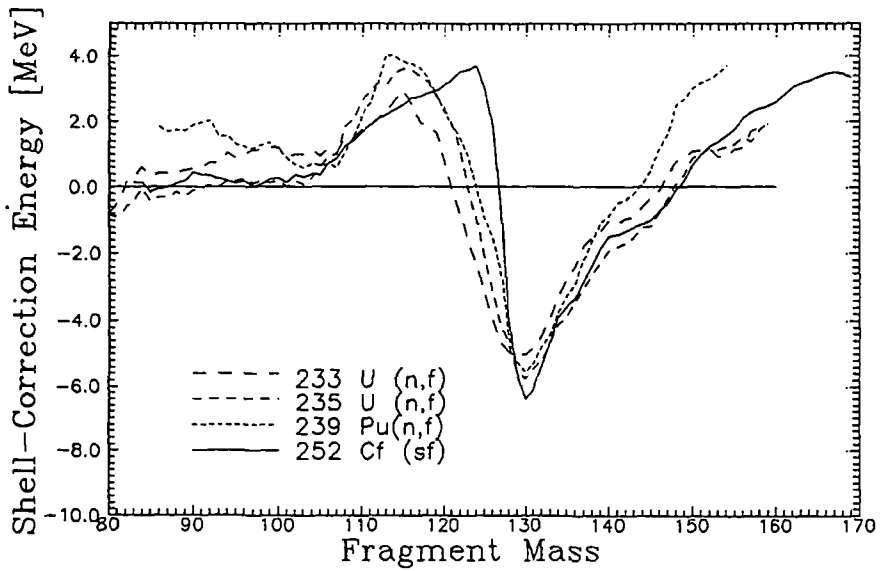

Fig.2 Calculated semi-empirical shell correction energies (τ=0) for different fission reaction ($\bar{\nu}$ data taken from ref.[24], TKE(A_1/A_2) from ref.[13,14])

intrinsic excitation, fission fragment energies and, consequently, neutron multiplicities can be obtained for any fission reaction in the actinide region.

V. DISSIPATIVE ENERGY IN SPONTANEOUS AND INDUCED FISSION

A relative vacant problem in nuclear fission is the decrease of potential energy between saddle and scission point. A wide range of possible values of the dissipative and the pre-scission kinetic energy between 0 and 50 MeV was given up to now. One method to deduce E_{dis} was presented by Gönnenwein[15]. Analyzing the proton pairing effect δ_p he has estimated dissipative energies as increasing with the fissility Z^2/A from about 3 MeV in the case of Thorium up to 11 MeV for Californium.

First applications of the TSM have shown that the calculated energy partitions are rather sensitive to the dissipated energy assumed. In deducing the phenomenological δw-parameter set this quantity is calculated according to Gönnenwein based on experimental δ_p data;

$^{235}U(n_{th},f)$: δ_p = 25 %[15] ——> E_{dis} = 6.2 MeV

$^{252}Cf(sf)$: δ_p = 12.1 %[16] ——> E_{dis} = 9.6 MeV

It has been found that an approximative parameterization of Gönnenwein's E_{dis} data for any TSM applications is not reliable. Therefore, dissipative energies have been fitted for many fissioning nuclei. These data together with the energies deduced by Gönnenwein are plotted in Fig.3 for different fission reactions.

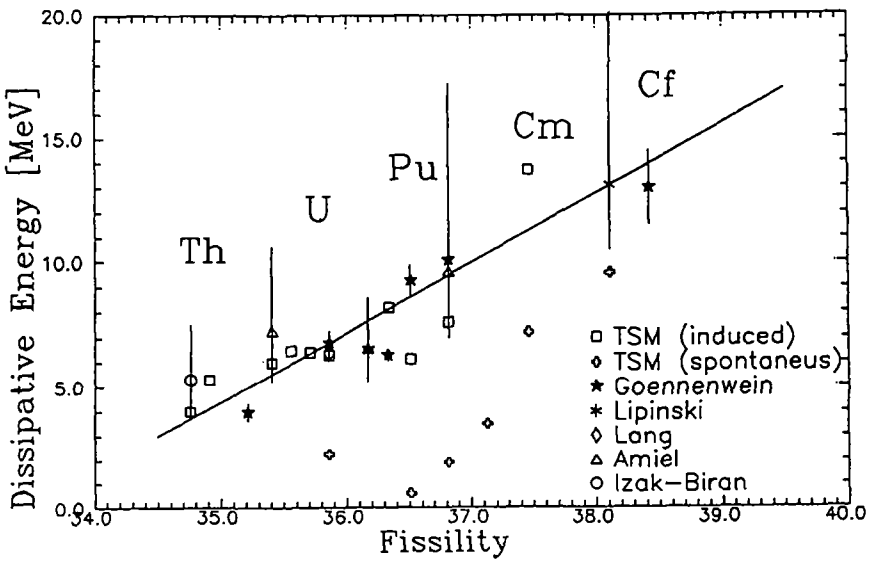

Fig.3 Fitted dissipative energies as function of fissility Z^2/A for different fission reaction in competition with the data deduced from proton odd-even effects by Gönnenwein[18] and deduced with δ_p data taken from ref.[19-22]

One might expect that ΔE_{pot} in the case of threshold fission with reference to spontaneous fission is enhanced by $E_{cn,thr}$, i.e. the compound nucleus excitation energy for threshold fission. Discussing the differences in E_{dis} and E_{pre}, we assume that the fragmentation process is separable into two phases:

1. Charge separation connected with rather strong friction: The main part of potential energy release is concentrated on E_{dis}.
2. Neck formation and rupture in conjunction with a pre-

acceleration of the nascent fragments: The potential release in this phase results E_{pre} mainly.

It is likely that differences between threshold and spontaneous (tunneling) fission concern the first phase predominantly, if ΔE_{pot} is sufficiently high. Even in this case, i.e. for $Z^2/A \geq 36$, $\overline{TKE}$ differences are very small. However for rather light fissioning nuclei ($Z^2/A \leq 36$), phase (2) is shifted close to barrier penetration in the case of spontaneous fission. E_{pre} and, consequently, $\overline{TKE}$ becomes lower compared to threshold fission.

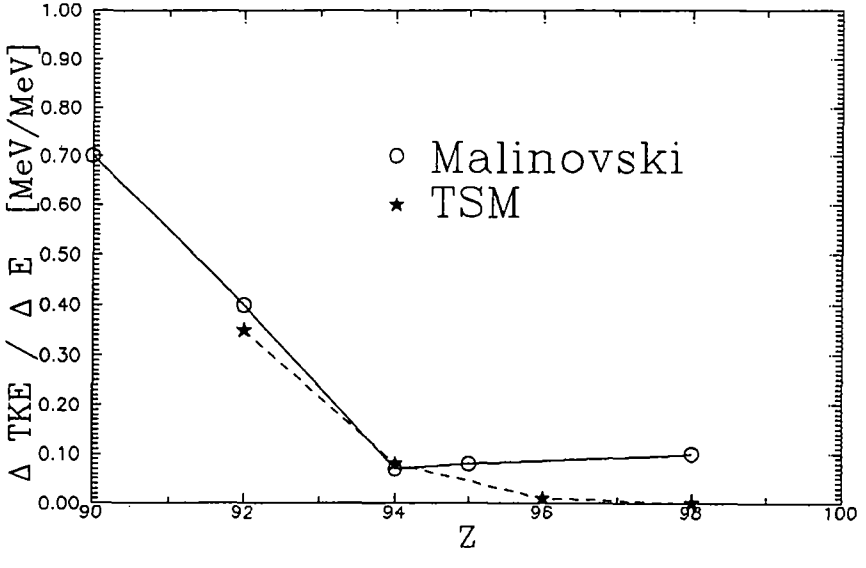

Fig.4 Change of TKE from spontaneous to threshold fission according to Malinovski[18] and fitted results obtained in the framework of TSM

Spontaneous fission compared with threshold fission exhibits a remarkable trend in changes of E_{dis} and E_{pre} (see Fig.4).
This interpretation is confirmed by the experimental-data trends. A remarkable difference in TKE between spontaneous and threshold fission, $\Delta\overline{TKE}$, exists only for nuclei lighter than Plutonium (cf. Fig.4). On the other hand, neutron multiplicity changes $\Delta\bar{\nu}$ (connected with E_{dis}) increase with the atomic mass of the fission nucleus as shown for instance by Gladkow[17].

VI RESULTS

VI.A. TOTAL KINETIC ENERGY OF FISSION FRAGMENTS

As shown in paragraph 2, the total kinetic energy as function of mass split is given by the sum of coulomb and pre-scission kinetic energy, where E_{pre} is approximated to Gönnenweins[15] values and E_{coul} is deduced from the minimization equations (equ.5,6) combined with the general energy balance (equ.1). Here, the knowledge of averaged Q-values $\bar{Q}(A_1/A_2)$ as the main part of the available energy is of special importance. These data are obtained on the basis of mass tables[23] considering an approximated charge distribution of fission fragments according to the results of Wahl[24].
The next figures show some typical examples of calculated $\overline{TKE}$ data in comparison with experimental results. Trends of changes in $\overline{TKE}$ with mass number and/or with incidence energy can be explained by the help of TSM as due to the influence of shell effects.
The total kinetic energy of two complementary fragments is essentially determined by the Coulomb repulsion. According to TSM, E_{coul} depends on the effective distance between the two fragment charges and consequently on fragment's deformation.
High negative shell correction energies (cf. Fig.2) are related to a strong stiffness. The nearly spherical shape of these fragments leads to a small distance between the charges. Thus, heavy fragments with mass number close to 132 which are characterized by extremely negative δw are connected with the maximum in $\overline{TKE}$. An increasing incidence energy diminishes this value because of decreasing stiffness due to the washing out of shell effects.
In the symmetric mass region the fragments with positive shell correction energies are quite soft concerning deformability. Since the centers of charges are far separated TKE is rather low. In this case, the diminution of shell effects is connected with smaller shell energies. Therefore, the stiffness and the kinetic energy increase with incidence energy.
The dependence of $\overline{TKE}$ on incidence energy and fragment mass is shown in Fig.5 where $\overline{TKE}$ changes $\Delta TKE(E_i,A)=TKE(E_i,A)-TKE(thermal,A)$ with reference to thermal neutron induced fission is plotted as function of fragment mass for 3 different incidence energies in the neutron induced fission of ^{235}U. The results are in good agreement with the experimental data measured by Straede[25].

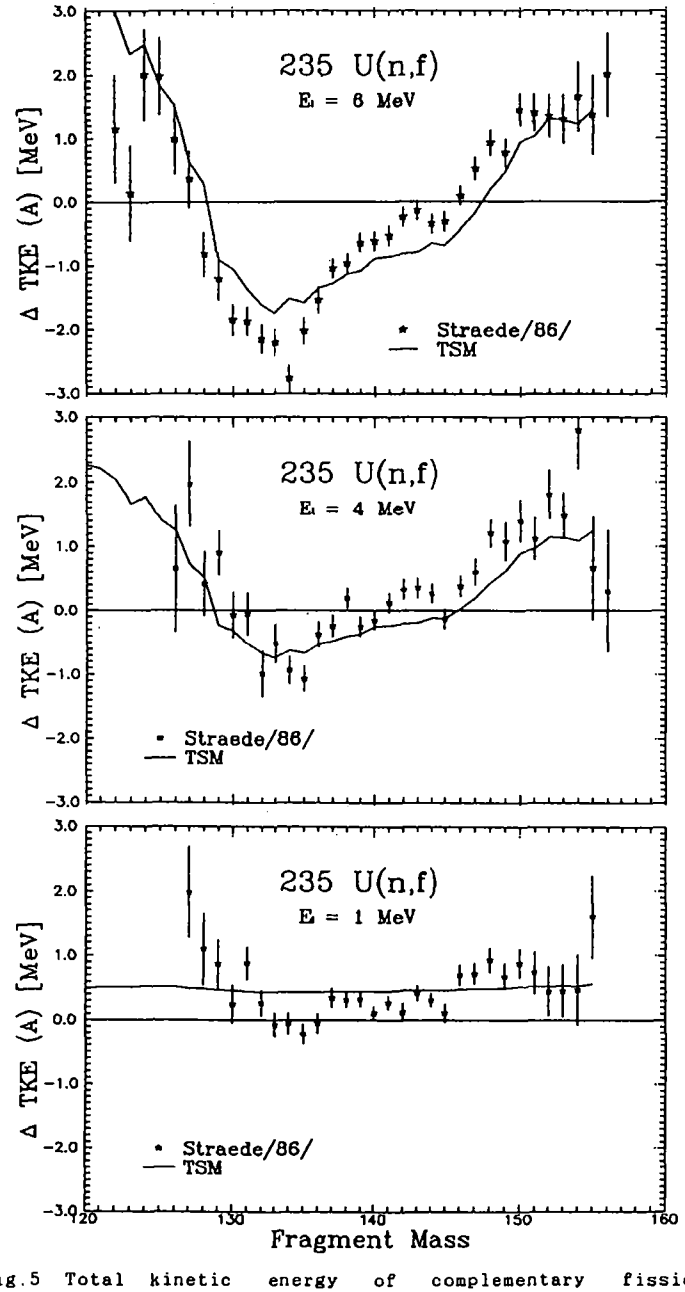

Fig.5 Total kinetic energy of complementary fission fragments of $^{235}U(n,f)$ for 3 different incidence energies plotted as difference to the value for thermal neutron induced fission (line - TSM, points - Straede[25])

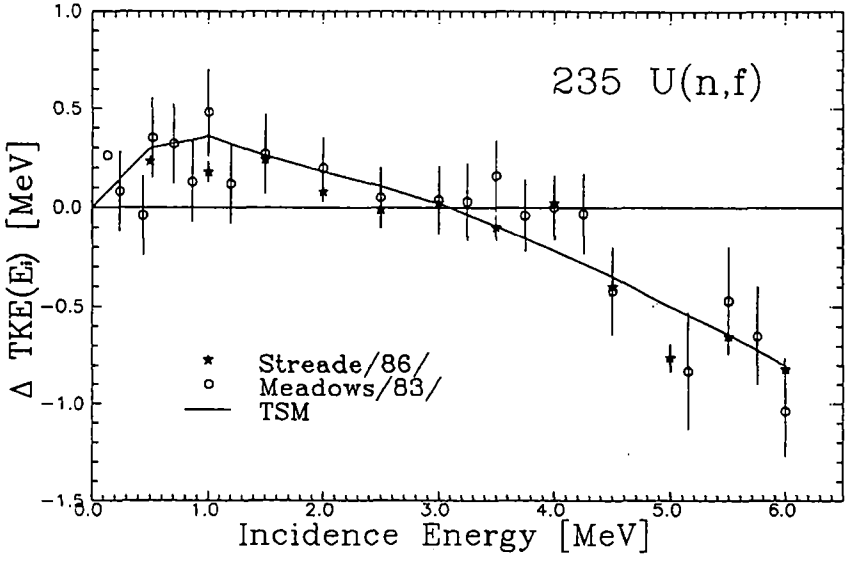

Fig.6 Averaged total kinetic energy as function of incidence energy for $^{235}U(n,f)$ plotted as difference for the value of thermal neutron induced fission. (line - TSM, points - Straede[25])

A special point to note is the general increase of TKE in the whole mass region in the case of E_i=1MeV. As shown in Fig.6 this increase is connected with a maximum of the average total kinetic energy,

$$\overline{TKE}(E_i) = \sum TKE(E_i,A_1/A_2)\ Y(E_i,A_1/A_2) \qquad (14)$$

($Y(E_i,A_1/A_2)$ - fragment mass yield) for given incidence energy. This behaviour of $\overline{TKE}$ for small incidence energy differs for various fission reactions (cf. Fig.7). In the framework of TSM, these changes in $\overline{TKE}$ are caused by alterations in the heat energy above the second fission barrier due to pair breaking. As introduced in chapter 2 (cf. Eq.2) the available intrinsic excitation energy is reduced by the pairing gap for odd-even, even-odd and especially for even-even fissioning nuclei. If the available energy above barrier, i.e. $\tilde{E}_h=E_{cn}+B_i+E_i-E_{f,b}$, is lower than the pairing gap Δ_p, the heat energy E_h is additionally reduced by Δ_p, which is a function of saddle point temperature[10]. Until the energy $\tilde{E}_h=\Delta_p$, increasing incidence energy gives rise to a higher kinetic energy of the fission fragments.

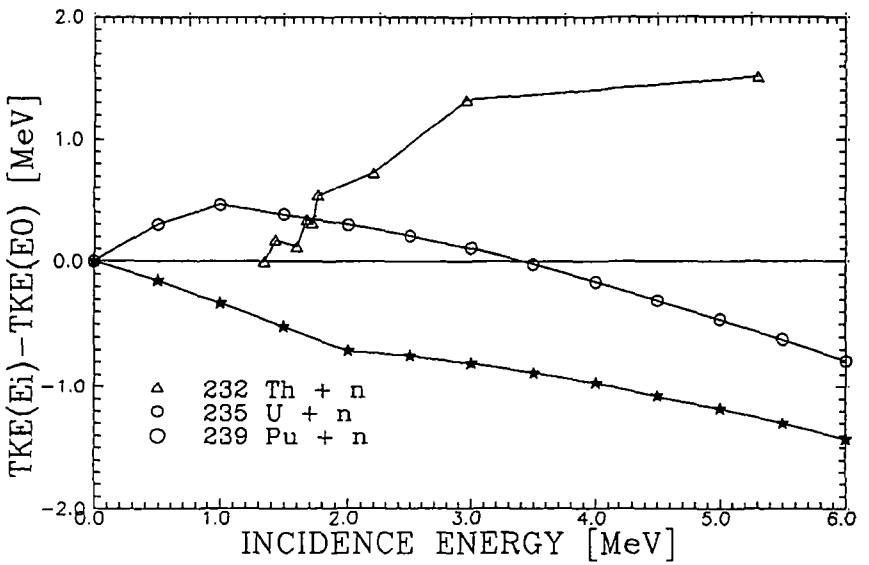

Fig.7 Calculated average total kinetic energy $\overline{TKE}(E_i)$ as difference to the value of minimum (thermal or threshold) incidence energy for different incidence energies and various fission nuclei

Above it, $\overline{TKE}(E_i)$ decrease with E_i as the result of the temperature dependence of the shell energies.

It is emphasized that the barrier structure differs for the fissioning nuclei studied in this work systematically. In particular, $E_{f,A} < E_{f,B}$ for $A \leq 235$ and $E_{f,A} > E_{f,B}$ for $A \geq 238$

The higher value determines the effective fission threshold. For the fissioning nuclei ^{233}Th, ^{236}U and ^{240}u considered in Fig. 7, the barrier values $E_{f,A}$ / $E_{f,B}$ are[26] :

6.55 / 6.65 MeV

5.63 / 5.53 MeV and

5.57 / 5.07 MeV, respectively.

Obviously, the influence of pairing on energy partition as function of incidence energy is minor or negligible, if $E_{f,A}$ is remarkably higher then $E_{f,B}$. This is the case for Pu-fission. The compound nucleus excitation energy for thermal neutron induced fission is 6.52 MeV[26] compared to the 5.07 MeV barrier B. Here, pairing at saddle doesn't play any significant role. $\overline{TKE}$ decreases as function of neutron incidence energy in the full energy range considered.

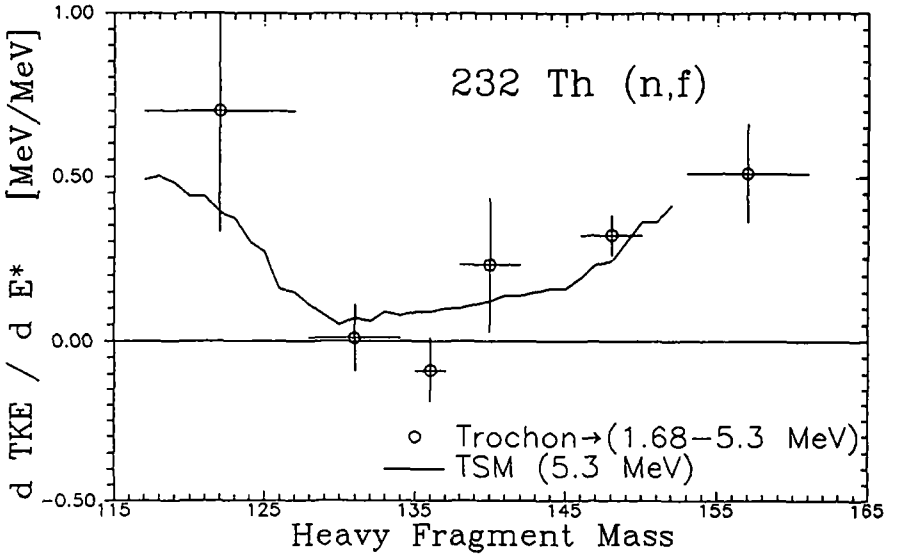

Fig.8 Total kinetic energy as difference to the value of threshold fission plotted as function of the heavy fragment mass (solid line - TSM E_i=5.8 MeV, points - averaged values for E_i= 1.72, 1.77, 2.2, 2.96 and 5.3 MeV according to Trochon[27])

The $^{232}Th(n,f)$ reaction has the opposite behaviour at low incidence energy. Further a shift of the most probable mass in the mass yield for $E_i > 3$MeV towards fragments with higher kinetic energies (cf. ref.[27]) leads to an increasing $\overline{TKE}(E_i)$ above 3 MeV incidence energy as shown in Fig.7 in the Th-case.

Fig. 8 illustrates this assumption showing the fragment mass dependence of TKE. The plotted experimental points[27] are summed values for incidence energies 1.72, 1.77, 2.2, 2.96 and 5.9 MeV.

VI.B. THE AVERAGE NEUTRON MULTIPLICITY

To deduce the neutron multiplicity of fission fragments an energy balance of fragment de-excitation is proposed including the evaporation of neutrons (multiplicity $\bar{\nu}$, average CMS energy $\bar{\varepsilon}$) and γ-ray emission (average total energy $\bar{E}_\gamma$),

$$\bar{E}^*(A_i) = \bar{\nu}(A_i)\,(\bar{B}_n(A_i) + \bar{\varepsilon}(A_i)) + \bar{E}_\gamma(A_i). \qquad (15)$$

The average neutron separation energy is calculated on the basis of mass tables[29] using an approximated charge distribution according to Wahl[24] ($\rightarrow \bar{B}_n^{z\text{-dis}}(A)$). To consider the increase of $\bar{B}_n(A)$ with $\bar{\nu}$ due to the shift of the fission fragments towards the line of β-stability these data are corrected according to,

$$\bar{B}_n(A) = \bar{B}_n^{z\text{-dis}}(A) + C\ \bar{\nu}(A) \qquad (16)$$

with the correction factor C (0.1-Uranium ...0.3-Californium).
According to the results of Frehaut[28] the average total gamma energy is assumed to be linear in the neutron multiplicity. Thus, $\bar{E}_\gamma(A_i)$ is given in the Th-Cf region by the following approximation,

$$\bar{E}_\gamma(A) = [\ G_1\ \bar{\nu}(A) + 2.2\ ]\ \text{MeV} \qquad (17)$$

The constant G_1, which depends on the mass of the fissioning nucleus as depicted in Fig. 9, is taken from Frehaut[28].
In the next figure calculated neutron multiplicities as a function of fragment mass are shown for two different incidence energies (0.8 and 5.55 MeV) for the neutron induced fission of ^{237}Np. The plotted experimental data were taken from Müller[29].
In the framework of the TSM, the saw-tooth curve of neutron multiplicity corresponds to the shell structure of the fragments. After scission the deformation energy is dissipated into excitation energy which give rise to neutron emission. Therefore, fragments with a large deformation (positive δw) cause a high number of evaporated neutrons. On the other hand the negative shell correction energies of the heavy fragments lead to a dip in the $\bar{\nu}(A)$ curve.
Both experimental and calculated data show that differences in $\bar{\nu}(A)$ with increasing incidence energy exist in the region of heavy fragments (125<A<145) mainly. As shown in Fig.2 these fragments are characterized by extremely (negative) shell correction energies which are especially changed due to intrinsic excitation.
A last remarkable test of the accuracy of description of energy partition and neutron emission with the TSM is the dependence of neutron multiplicity averaged over all fragments on incidence energy. The last three figures show this behaviour for three different fission reactions. In the case of Thorium (Fig.11) this investigation includes both (n,f) and (n,n'f) reactions. To account for multiple chance fission, in general (n,jnf), the

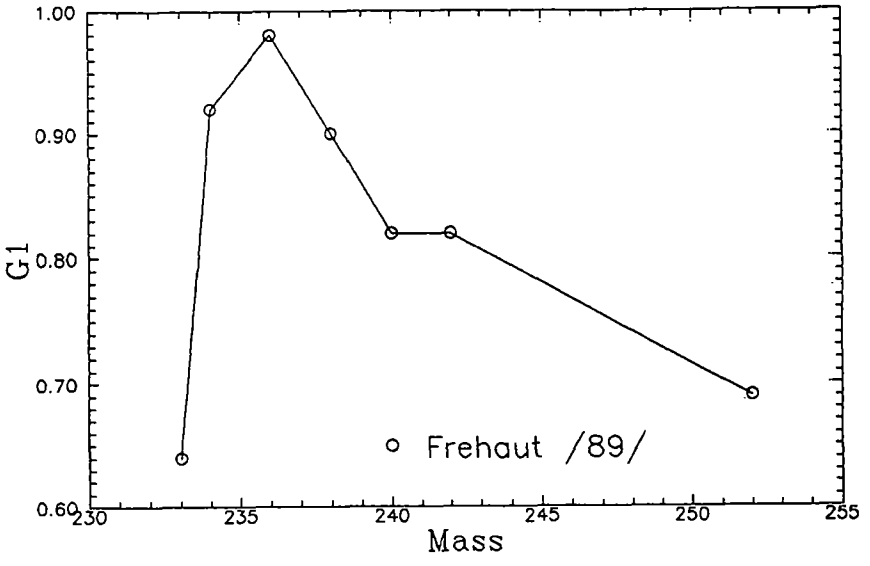

Fig.9 Constant G_1 for relation between average total γ-energy and average neutron multiplicity as function of mass of fissioning nucleus according to Frehaut[29]

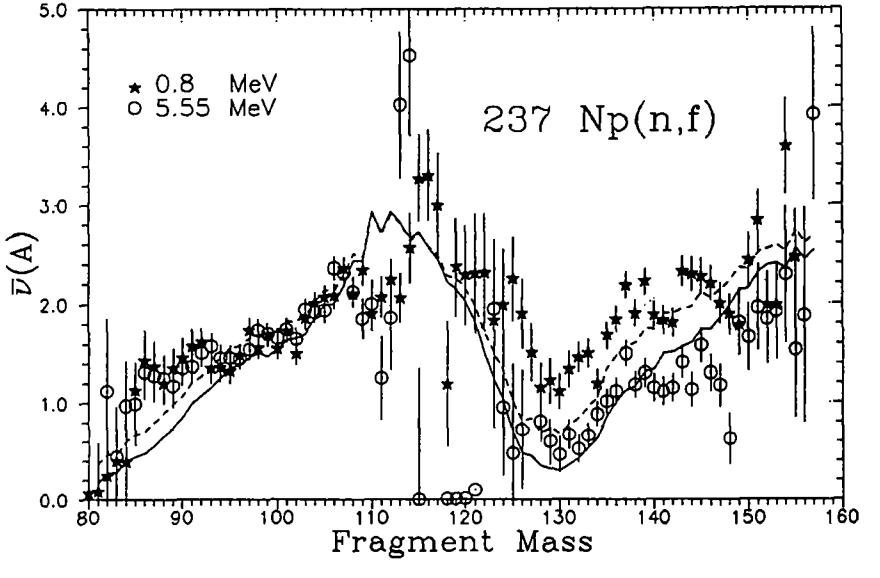

Fig.10 Calculated neutron multiplicity as function of fragment mass in comparision with experimental data[29] for the ^{237}Np(n,f) reaction

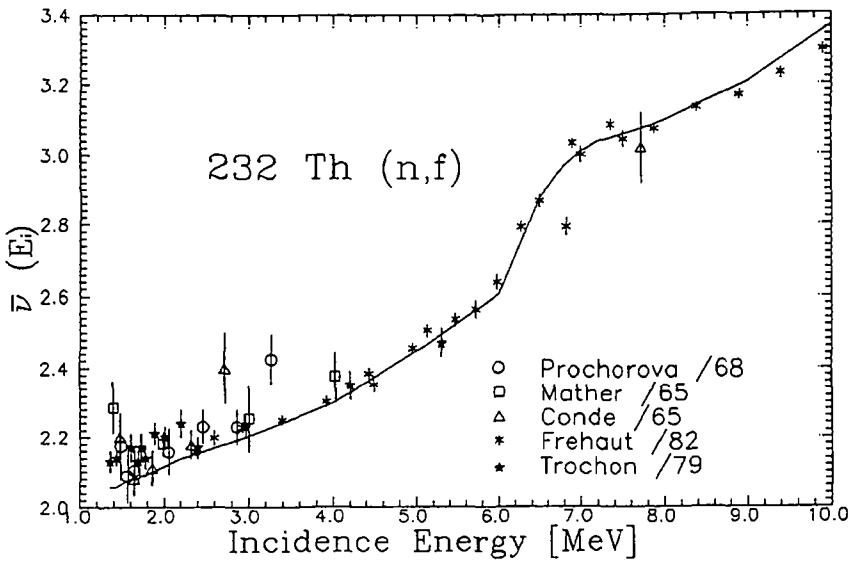

Fig.11 Average neutron multiplicity as function of incidence energy for the neutron induced fission of ^{232}Th (experimental data were taken from ref.:[27,90-96])

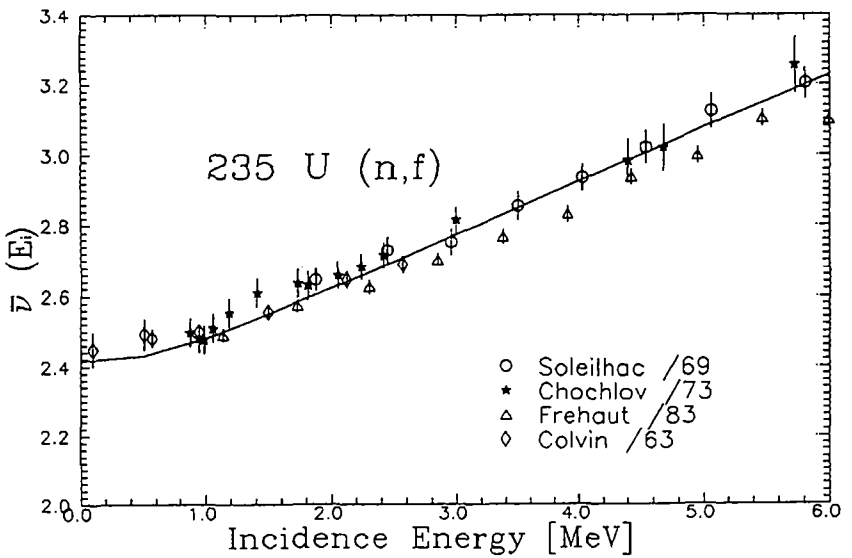

Fig.12 Average neutron multiplicity as function of incidence energy for ^{235}U(n,f) (experimental data were taken from ref.[89-96])

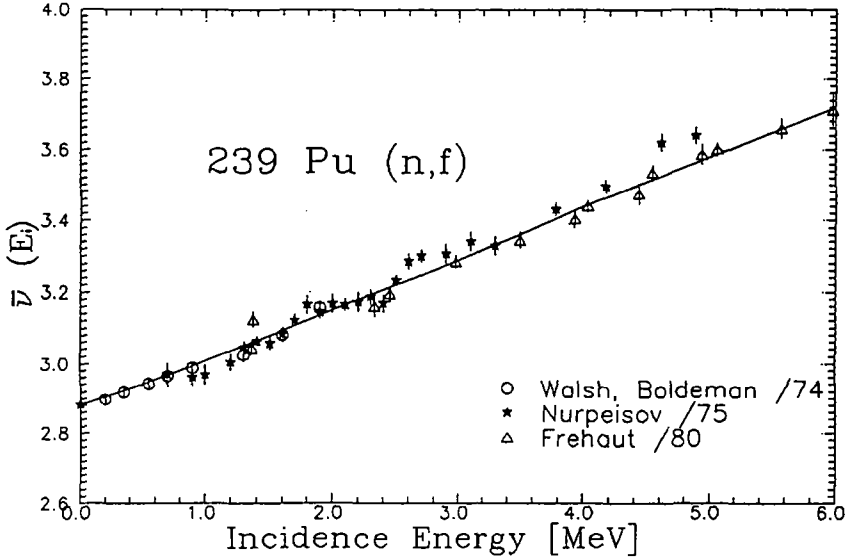

Fig.13 Average neutron multiplicity as function of incidence energy for ^{239}Pu(n,f) (experimental data were taken from ref.[87-89])

neutron multiplicities $\bar{\nu}_j(E_i)$ for both reactions have been calculated and added considering the partial fission cross sections $\sigma_{f,j}(E_i)$ of chance j,

$$\bar{\nu}_{tot}(E_i) = \frac{\sum_{j=0}^{j_{max}} \bar{\nu}_j(E_i)\ \sigma_{f,j}(E_i)}{\sigma_{f,tot}} \qquad (17)$$

The bend in the $\bar{\nu}(E_i)$ curve above 6 MeV incidence energy is a consequence of second chance fission characterized by lower $\overline{TKE}$ as in the first chance case and consequently, higher $\bar{\nu}$ values. The TSM calculation reproduces the experimental data.

Fig. 12 and 13 show a similar investigation as discussed above for neutron induced fission of ^{235}U and ^{239}Pu for the first chance emission (n,f). Even these figures show a good agreement between measured and calculated data.

VII. SUMMARY AND CONCLUSIONS

The TSM as a scission point model with semi-empirical, temperature-dependent shell correction energies for deformed fragments at scission is successful in describing the main features of energy partition in fission as function of mass asymmetry. The diminution of shell effects due to scission point temperature, which depends on the dissipated energy as well as incidence energy (influenced by pairing effects), cause considerable changes of fragment energies as function of incidence energy.

Remarkable changes in the fragment energies between spontaneous and threshold fission are explained by the TSM as an effect of systematic alterations in the dissipated and pre-scission kinetic energy. Fitting the calculated fragment data dissipative energies for both types of fission reaction have been obtained.

The average fragment excitation energy has been used used to obtain neutron multiplicity by the help of an energy balance of fragment de-excitation, which includes neutron evaporation and γ-ray emission. The typical saw-tooth in the $\bar{\nu}(A)$ curve as well as the dependence of $\bar{\nu}$ on incidence energy is reproduced by the TSM with good accuracy.

The TSM provides the basis for several applications as the calculation of fragment data as well as neutron emission probabilities. This model will be used for corresponding data systematics in next future.

REFERENCES

1. J. Moreau and K. Heyde, manuscript "Theoretical models of mass distributions", to be published in "Nuclear Fission Review", ed. by C. Waagemans
2. N.Bohr and J.Wheeler, Phys. Rev 56, 426 (1939)
3. W.Brunner and H.Paul, Ann.d.Phys.7, 326 (1961)
4. R.Vandenbosch, Nucl.Phys.46, 129 (1963)
5. J. Terrell, Proc. IAEA Symp. on Phys. and Chem. of Fission, Salzburg, 1965 (Vienna, 1965) Vol. II, p. 3
6. M. Kildir and N.K. Aras, Phys. Rev. C25, 365 (1982)
7. W.D.Myers and W.J.Swiatecki, Nucl.Phys.81, 1 (1966)
8. B.D. Wilkins et al., Phys. Rev. C14, 1832 (1976)
9. U.Brosa et al., Proc. XVIth Int. Symp. on Nucl. Phys., Gaussig (GDR), 1986, ZfK-610, 162 (1986)
10. J. Kristiak, Proc. 5th Int. Symp. on Neutron Induced Reactions, Smolenice, 1988, in print
11. A. Bohr and B.R. Mottelson, "Nuclear Structure" (Benjamin, New York, 1975), vol. II
12. A. V. Ignatjuk et al., Yad. Fiz. 42 /, 569 (1985)
13. W. F. Apalin et al., Nucl. Phys. 71, 553 (1965)
14. R. Schmidt-Fabian, PhD Thesis,"Messung der spontanen Spaltung von ^{252}Cf am Darmstadt - Heidelberger - Kristallkugel - Spektrometer", (1988) Ruprecht-Karls-Universität Heidelberg
15. F. Gönnenwein et al., Proc. XVIIth Int. Symp. on Nucl. Phys., Gaussig (GDR), 1987, ZfK-646, 129 (1988)
16. T. Datta et al., Proc. XVIIIth Int. Symp. on Nucl. Phys., Gaussig (GDR), 1988, in print
17. W. W. Gladkov et al., Yad. Const. 1(40), 48 (1981),
18. W. W. Malinovski, Jad. Konst. 2, 25 (1987),
19. R. J. Lipinsk and B. W. Wehring, Phys.Lett. 66B, 326 (1977)
20. W. Lang, PhD Thesis, "Nuklidausbeuten bei der Reaktion ^{235}U(n_{th},f) als Funktion der kinetischen Energie der Spaltprodukte - Ein experimenteller Zugang zur Dynamik des Spaltprozesses", TH Darmstadt (1979)
21. S. Amiel et al., Phys. Rev. C15, 2119 (1977)
22. T. Izak-Biran and S. Amiel, Phys. Rev. 96, 1059 (1954)
23. Y. Ando et al., JAERI-M83-025
24. A. C. Wahl, Atomic Data and Nuclear Data Tables 39, 1 (1988)
25. C. A. Straede et al., Nucl. Phys. A462, 85 (1987)
26. S. Bjornholm and J. E. Lynn, Rev. Mod. Phys. 52, No.4, 725 (1980)
27. J. Trochon et al., Nucl. Phys. A318, 63 (1979)
28. J. Frehaut, Proc. of Cons. Meeting on Physics of Neutron Emission in Fission, Mito 19888, IAEA Wien, 1989, INDC(NDS)-220, 99
29. K. Müller et al., "Numerical results of a (2E,2v) - measurement for fast neutron induced fission of ^{235}U and ^{237}Np", KFK - Berichte 3220 (1981)
30. L. I. Prochorova et al., Sov. J. Nucl. Energy 7, 579 (1968)
31. D. S. Mather et al., Nucl. Phys. 66, 149 (1965)
32. H. Conde et al., Arkiv Phys. 29, 33 (1965)
33. J. Frehaut et al., Proc. of Intern. Conf. on Nucl. Data for Science and Technology, 6-10 Sept. 1982, Antwerpen D. Reidel Publishing Company, 78 (1983)

34. M. Soleilhac et al., Nucl. Energy 23, 257 (1969)
35. J. A. Chochlov et al., Proc. IIIth Conf. on Neutron Phys., Kiev, 9-13 June, ZNII Atominform, V, 186 (1976)
36. D. W. Colvin and M. G. Sowerby, in R. J. Howerton, Nucl. Sci and Eng., 62, 438 (1977)
37. B. L. Walsh and J. W. Boldeman, Ann. Nucl. Sci. Engng. 1, 353 (1974)
38. B. Nurpeisov et al., At. Energy 39 /3, 199 (1975)
39 J. Frehaut et al., "Recent results on ν-prompt measurements between 1.5 and 15 MeV", Paris 1980